Journal of Rajasthan Academy of Physical Sciences
ISSN: 0972-6306; URL: http://raops.org.in
Vol.21, No.1&2, January-June, 2022, 71-82

MAGNETIC FIELD EFFECT ON NANOFLUID FLOW TOWARDS A STRETCH SHEET FILLED IN POROUS MEDIUM

NVN Babu[1], Murali G[2], Sanjay Ch[3], Chandu. M.Koli[3]
[1]Department of Engineering Science, Sanjivani College of Engineering, Kopargaon, India.
[2]Department of Mathematics, Malla Reddy Univrersity, Hyderabad,India.
[3]Department of applied Science, SVKM Institute of Techonology, Dhule, India.

Abstract. The aim of the research study is about the magnetic field effect and porous medium on non-newtonian nanofluid, in the presence of variable viscosity and convective boundary condition that flows in the direction of a stretching sheet. During this study, nanofluid model is used for the effects of thermophoresis and Brownian motion. Using suitable transformations, the basic governing coupled non-linear partial differential equations for velocity (momentum), temperature (energy) and nanoparticles concentration are reduced into a group of non-linear ordinary differential equations. The resultant transformed equations are solved numerically using fourth-fifth order Runge-Kutta-Fehlberg method. The consequences of various engineering parameters on the dimensionless velocity, temperature, nanoparticles concentration profiles are discussed and presented graphically. Also, the numerical values of skin-friction, rate of heat and mass transfer coefficients are presented in tabular forms. The earlier published results have the similarity with the obtained numerical results as special cases of the earlier study.

Keywords: Nanofluid flow; Stretching Sheet; Magnetic field; Porous Medium; Numerical Solutions.

1. Introduction

Normally, natural convection boundary layer flow, heat and mass transfer problems involving heating condition all alongside the boundary of the surface that forms a solid-fluid interface be recommended frequently. Maintaining an even temperature or an even heat flux are used as a common condition. General, there's an issue that arises that what surface boundary condition has got to be implemented on the surface temperature. In spite of using an even temperature or an even heat flux as a repetitive boundary condition, it ascends in practice as there is more thermal conductivity to the porous medium in the solid body. It is similar to say that the Biot number of the problem has a finite value and is not equivalent to zero. In real applications the Biot number has a finite value and, seldom, the thermal boundary conditions may be known in advance. Not a prescribed temperature or heat flux will appear completely suitable, a convective condition, being in essence a combination of those two conditions, is moreover realizable in practice and it

should provide further useful insights. Makinde and Aziz [11] studied the effect of convective boundary condition on nanofluid flow past a stretching sheet. Nadeem et al. [13] studied the effect of partial slip on stagnation point over a nanofluid towards a stretching surface in presence of convective boundary condition. Ibanez [5] studied magnetohydrodynamic flow past a porous channel with Entropy generation and the condition of convective boundary. Reddy et al. [15] studied mixed convective flow of nanofluid in presence of convective boundary condition and thermal diffusion effects. Hayat et al. [4] studied on an instablehydromagnetic free convective flow over an infinite vertical plate embedded in a porous medium with heat absorption is caused by heat and mass transfer. Paul et al. [14] discussed the effects of magnetic field and convective boundary condition on 3D flow in presence of couple stress nanofluid past a non-linearly stretching surface. Khan and Pop, Mahanthesh et al. [7,9,10] studied the thermal radiative flow of magneto water based nanofluid past a nonlinearly stretching surface with convective boundary condition. Hayat et al. [4] studied stagnation point over a hyperbolic tangent nanofluid flow with convective conditions. Aziz [1] found the similarity solutions on a flat plate with a convective surface boundary condition. Ishak [6] found analytical solutions for heat transfer flow through aabsorptive surface with convective boundary condition. Lopez et al. [8] and Buongiorno [2] discussed Entropy generation analysis of MHD nanofluid flow in a porous vertical micro channel with convective-radiative boundary conditions. Murali et al.[12], Gora and Sidawi [3] and Wang [16] studied, Heat and Mass Transfer with Free Convection MHD Flow past a Vertical porous Plate: Numerical study.

Motivated by the above reference work, the main theme of present article is to study the combined influence of magnetic field and porous medium on non-newtonian nanofluid flow over a nonlinear stretching surface with variable viscosity and convective boundary condition. For this study, Brownian motion and thermophoresis effects are studied. The non-linear system is computed through the implementation of fourth-fifth order Runge-Kutta-Fehlberg method. The flow components like fluid velocity, fluid temperature and nanoparticle concentration profiles are graphically sketched for various governing parameters.

2. Mathematical formulation

In this present research work, steady, two-dimensional, viscous, incompressible, electrically conducting, laminar flow of a Nanofluid through a stretching surface when magnetic field exists, porous medium and convective boundary condition are considered. The geometrical structure of this research work is presented in Fig. 1. The following assumptions be made used for investigation.

i. The stretching sheet is protracted with a velocity $u_w = ax$ with static source place, where a is a real positive number and x is the coordinate measured along the stretching surface.

ii. The stretching surface is maintained at prescribed surface temperature $T = T_w$ to be decided after, is the result of a characterized convective heating process by a temperature T_f and heat transfer coefficient h.

iii. The nano particle volume fraction C at the wall is C_w as at larger values of y, the value is C_∞.

iv. Induced magnetic field is assumed to be small as compared to applied magnetic field and is neglected.

v. The Buongiorno's [2] model may be modified for this problem to give the following continuity, momentum, energy and volume fraction equations.

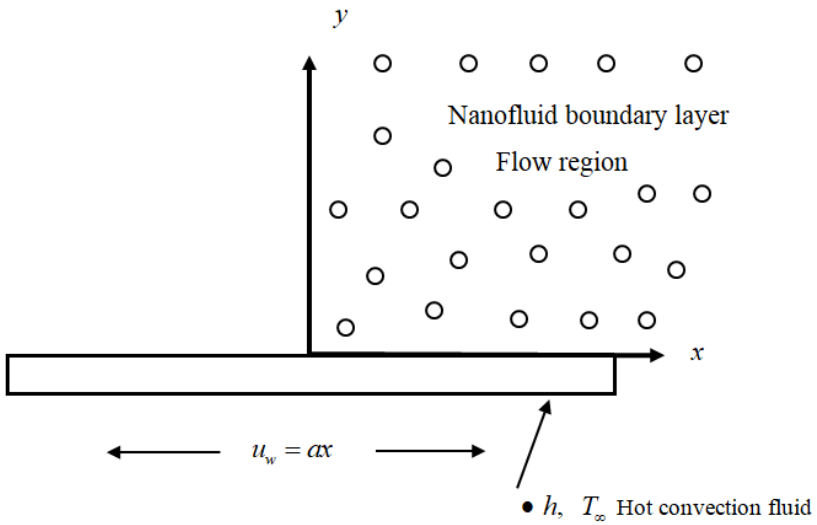

Fig. 1: Geometry of the problem

Continuity Equation:

$$\left(\frac{\partial u}{\partial x}\right)+\left(\frac{\partial v}{\partial y}\right)=0 \tag{1}$$

Momentum Equation:

$$u\left(\frac{\partial u}{\partial x}\right)+v\left(\frac{\partial u}{\partial y}\right)=-\frac{1}{\rho_f}\left(\frac{\partial p}{\partial x}\right)+\nu\left(\frac{\partial^2 u}{\partial x^2}+\frac{\partial^2 u}{\partial y^2}\right)-\left(\frac{\mu}{k^*}\right)u-\left(\frac{\sigma B_o^2}{\rho_f}\right)u \tag{2}$$

$$u\left(\frac{\partial v}{\partial x}\right)+v\left(\frac{\partial v}{\partial y}\right)=-\frac{1}{\rho_f}\left(\frac{\partial p}{\partial y}\right)+\nu\left(\frac{\partial^2 v}{\partial x^2}+\frac{\partial^2 v}{\partial y^2}\right) \tag{3}$$

Equation of thermal energy:

$$u\left(\frac{\partial T}{\partial x}\right)+v\left(\frac{\partial T}{\partial y}\right)=\alpha\left(\frac{\partial^2 T}{\partial x^2}+\frac{\partial^2 T}{\partial y^2}\right)+\tau\left\{D_B\left(\left(\frac{\partial T}{\partial x}\right)\left(\frac{\partial C}{\partial x}\right)+\left(\frac{\partial T}{\partial y}\right)\left(\frac{\partial C}{\partial y}\right)\right)+\left(\frac{D_T}{T_\infty}\right)\left(\left(\frac{\partial T}{\partial x}\right)^2+\left(\frac{\partial T}{\partial y}\right)^2\right)\right\} \quad (4)$$

Equation of nanoparticles concentration:

$$u\left(\frac{\partial C}{\partial x}\right)+v\left(\frac{\partial C}{\partial y}\right)=D_B\left(\frac{\partial^2 C}{\partial x^2}+\frac{\partial^2 C}{\partial y^2}\right)+\left(\frac{D_T}{T_\infty}\right)\left(\frac{\partial^2 T}{\partial x^2}+\frac{\partial^2 T}{\partial y^2}\right) \quad (5)$$

For this flow, the appropriate boundary conditions are

$$\left.\begin{array}{l} u=ax,\ v=0,\ -k\left(\dfrac{\partial T}{\partial y}\right)=h\left(T_f-T\right),\ C=C_w\ at\ \ y=0\ \&\ u\to 0,\ T\to T_\infty,\ C\to C_\infty\ as\ \ y\to\infty \end{array}\right\} \quad (6)$$

By using similarity transformations

$$\left.\begin{array}{l} \eta=y\sqrt{\left(\dfrac{a}{\nu}\right)},\ \psi=\left(\sqrt{a\nu}\right)xf\left(\eta\right),\ \theta\left(\eta\right)=\dfrac{T-T_\infty}{T_f-T_\infty},\ \varphi\left(\eta\right)=\dfrac{C-C_\infty}{C_w-C_\infty} \end{array}\right\} \quad (7)$$

Where ψ is the stream function with $u=\dfrac{\partial\psi}{\partial y}$, $v=-\dfrac{\partial\psi}{\partial x}$ and $f'=\dfrac{u}{u_w}=\dfrac{u}{ax}$. The continuity is thus identically satisfied. An order of magnitude analysis of the $y-$ direction momentum equation (normal to the stretching sheet) using the usual boundary layer approximations $u>>v\ \Rightarrow\dfrac{\partial u}{\partial y}>>\dfrac{\partial u}{\partial x}.\dfrac{\partial v}{\partial x}.\dfrac{\partial v}{\partial y}$ shows that $\dfrac{\partial p}{\partial y}=0$. Thus neglecting the pressure gradient in the $y-$direction, the momentum, energy and volume fraction (concentration) equations and the boundary conditions reduce to the following system of equations.

$$f'''+ff''-f'^2-\left(M+K\right)f'=0 \quad (8)$$

$$\theta''+\Pr f\theta'+\Pr Nb\varphi'\theta'+\Pr Nt\theta'^2=0 \quad (9)$$

$$\varphi''+Lef\varphi'+\frac{Nt}{Nb}\theta''=0 \quad (10)$$

and the following boundary conditions (6) become

$$\left.\begin{array}{l} f\left(0\right)=0,\ f'\left(0\right)=1,\ \theta'\left(0\right)=-Bi\left[1-\theta\left(0\right)\right],\ \varphi\left(0\right)=1 \\ f'\to 0,\ \theta\to 0,\ \varphi\to 0\ as\ \eta\to\infty \end{array}\right\} \quad (11)$$

Where prime denotes differentiation with respect to η, the involved physical parameters are defined as follows

$$\left.\begin{aligned} &\mathrm{Pr}=\frac{\nu}{\alpha},\ Le=\frac{\nu}{D_B},\ Nb=\frac{(\rho c)_p D_B(C_w-C_\infty)}{(\rho c)_f \nu},\ Nt=\frac{(\rho c)_p D_T(T_f-T_\infty)}{(\rho c)_f \nu T_\infty},\ Bi=\frac{hx}{k}\sqrt{\frac{\nu}{a}},\\ &M=\frac{\sigma B_o^2}{a\rho},\ K=\frac{ak^*}{\mu} \end{aligned}\right\} \quad (12)$$

Quantities of functionalconcern in this challenge are the skin-friction coefficient (*Cf*), local Nusselt number (Nu_x), and the local Sherwood number (Sh_x), that are well-defined as

$$Cf=\frac{2\tau_w}{\rho},\ Nu_x=\frac{q_w x}{k(T_w-T_\infty)},\ Sh_x=\frac{J_w x}{D_B(C_w-C_\infty)} \quad (13)$$

Where τ_w, q_w and J_w are the skin-friction, heat and mass fluxes at the surface respectively and these quantities are defined as

$$\tau_w=\mu\left(\frac{\partial u}{\partial y}\right)_{y=0},\ q_w=-k\left(\frac{\partial T}{\partial y}\right)_{y=0},\ J_w=-D_B\left(\frac{\partial C}{\partial y}\right)_{y=0} \quad (14)$$

Using Eqs. (13) and (14), the dimensionless skin-friction coefficient, wall heat and mass transfer rates are defined as

$$Cf=2\mathrm{Re}_x^{\frac{3}{4}} f''(0),\ Nu_x=-\mathrm{Re}_x^{\frac{-1}{4}}\theta'(0),\ Sh_x=-\mathrm{Re}_x^{\frac{-1}{4}}\phi'(0) \quad (15)$$

Where $\mathrm{Re}_x=\frac{u_w(x)x}{\nu}$.

3. Method of Solution

Numerical Solutions by Fourth-Fifth Order Runge-Kutta-Fehlberg Method:

Eq. (11) constitutes a two-point boundary value problem in the set of non-linear coupled differential Eqs. (8), (9), (10) by proper boundary conditions specified in. The equations be decidedly non-linear and thus cannot be explainedmethodically. So, by using the symbolic computer algebra software Maple 17, these equations are solved numerically. Runge-Kutta-Fehlberg method is used in this software to explain the boundary value problem. The step size and convergence criterion were chosenfor this study, to be 0.01 and 10−8, respectively. The asymptotic boundary condition in Eq. (11) was nearly estimatedusing the value of $\eta_{\max}$ = 5 as f

$$f'(0)=\theta(0)=\phi(0)=5 \quad (15)$$

The numerical results are very important in numerical solution of differential equations, validation to ensure accuracy, consistency as well as reliability. A fourth-fifth order Runge-Kutta-Fehlberg method is used to resolve the boundary value problems numerically. Its accuracy and robustness are confirmed by different researchers.

Comparison of present results with published results:

Table-1: Comparison of Nusselt number results with $M = K = Nb = Nt = 0$ and $Bi = 1000$.

Pr	Present results	Khan and Pop [12]	Wang [13]	Gorla and Sidawi [14]
0.07	0.06643821578	0.0663	0.0656	0.0656
0.20	0.16852206244	0.1691	0.1691	0.1691
0.70	0.44562215487	0.4539	0.5349	0.4539
2.00	0.90123326594	0.9114	0.9114	0.9114
7.00	1.88520014562	1.8954	1.8905	1.8954
20.0	3.34203362159	3.3539	3.3539	3.3539

The code validation of the present research problem is discussed in tables-1, 2 and 3 with the previous published results. Table-1 shows the comparison of present Nusselt number results with Khan and Pop [7], Wang [16] and Gorla and Sidawi [3] for different values of Pr when $M = K = Nb = Nt = 0$ and $Bi = 1000$. In tables 2 and 3, the comparison of Nusselt and Sherwood number results is discussed with Khan and Pop [7] for different values of *Nb* and *Nt* when $Le = \Pr = 20$ and $Bi \to \infty$. From these tables, it is concluded that besidesthe current results are in admirablecovenant, it alsoconfirms that the applied methodology is correct.

Table-2.: Comparison of Nusselt number results with $Le = \Pr = 20$ and $Bi \to \infty$.

Nb	*Nt*	Present results	Khan and Pop [12]
0.1	0.1	0.94221005487	0.9524
0.2	0.1	0.50555218845	0.5056
0.3	0.1	0.24663998744	0.2522
0.1	0.2	0.68200154489	0.6932
0.1	0.3	0.51302263408	0.5201

Table-3.: Comparison of Sherwood number results with $Le = \Pr = 20$ and $Bi \to \infty$.

Nb	*Nt*	Present results	Khan and Pop [12]
0.1	0.1	2.12882154789	2.1294
0.2	0.1	2.37620154625	2.3819
0.3	0.1	2.41002154872	2.4100
0.1	0.2	2.26920154862	2.2740
0.1	0.3	2.52031457867	2.5286

4. Results and Discussion

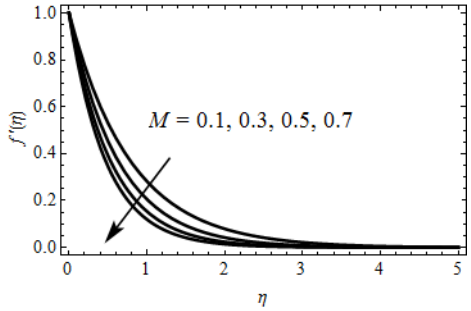

Fig. 2 *M* effect on Velocity profiles

This section presents the graphical results of various parameters arises within the fluid flow problem on the basis of a present study. "Maple 17" is used to analyze more vigorously the inclusions of Magnetic parameter or Hartmann number (M), Porous medium parameter (K), Thermophoresis parameter (Nt),Brownian motion parameter (*Nb*), Lewis number (*Le*), Prandtl number (Pr) and Biot number (*Bi*). Especially, we analyze their impacts on the distribution of temperature, velocity, and nanoparticle concentration profile. Within the subsequent figures, black coloured curves show the variations of given variable with the mentioned parameter in ascending and descending orders with the following of up and down arrow marks.

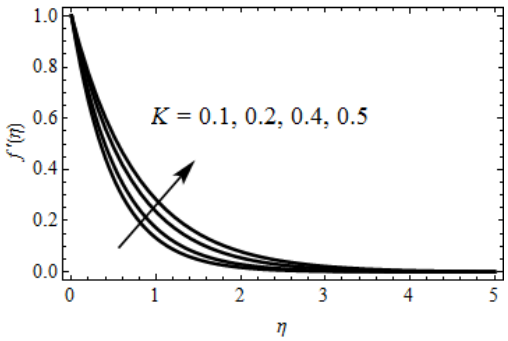

Fig. 3.*K* effect on Velocity profiles

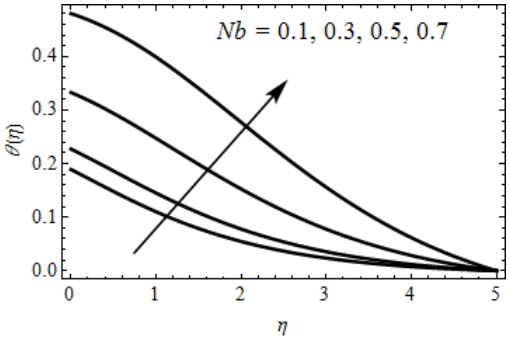

Fig. 4. *Nb* effect on Temperature profiles

The variation of Hartmann number (*M*) with $f'(\eta)$ is represented by Fig. 2. The displayed figure illustrates that the velocity profile lean towards weaken noticeablyfor higher values of Hartmann number (M). "Lorentz force" is produced by an opposing force that lessen the motion of the fluid, when the magnetic field is applied to electrically conducting fluid and create a notable resistance.

From Fig. 3, it is noted that an increase in the permeability parameter of the porous medium *K* enhances velocity profiles due to the less friction force. In fact, the resistance of the porous medium was reduced by higher values of K, as a result, the momentum development of the regime increases and resulting acceleration of the fluid flow in velocity profiles.

Fig. 4 and Fig. 5 shows that the behaviour of Brownian motion and thermophoresis effect on temperature profile. For higher values of thermophoresis parameter (*Nt*) temperature profile increases is shown in Fig. 4. Substantially, to analyze the temperature profile in various nanofluid flow problems, thermophoresis parameter is a primary source athermophoresis force was created by Higher impact of thermophoresis parameter (Nt). It is helped by Thermophoresisforce to escape the nanoparticles from a hot part to the cold part and boosts the temperature profile. Fig. 5 depicts that the temperature profile is boosted by Brownian motion parameter (*Nb*) significantly and its corresponding boundary layer thickness. Brownian motion was created due to the presence of nanoparticles and the Brownian motion is affected in various nanofluid flow problems, due the enhancement in Brownian motion (Nb) resulting concentration profile increase.

Fig. 6 is plotted for different values of Prandtl number (Pr) against temperature profile. In this figure we can see that an increment in Prandtl number (Pr) produces a marked reduction in the temperature distribution Higher values of Prandtl number (Pr) are relevant to lower thermal diffusivity and various kinds of fluid whichhavelesser thermal diffusivity results very low temperature. Owing to this lower thermal diffusivity, there is a decrement in temperature distribution.

Fig. 7 depicts the influence of Biot number (*Bi*) on temperature profiles. The temperature profiles uplifts in the entire fluid system as the values of Biot number (Bi) upsurges. As the Biot number (Bi) values improve there exist higher internal thermal resistance of the cone than the thermal boundary layer. The finding shows that the temperature of the fluid is enhanced in the boundary layer regime.

It is noticed from Fig. 8 that a major reduction is caused by Lewis number (*Le*) in the nanoparticle concentration distribution. Lewis number (Le) mainly subjects to the coefficient of Brownian diffusion. The decrease in the coefficient of Brownian diffusion thatdisplays a lesser nanoparticle concentration is highly contributed by Higher values of Lewis number.

Fig. 9 represents the graph of nanoparticle volume fraction $\phi(\eta)$ versus η. It shows that as thermophoresis parameter increases, the graph and nanoparticle volume fraction boundary layer thickness also increases. This shows that resistance to the diffusion of mass is induced by an increment in thermophoresis parameter.

The change in Brownian motion parameter *Nb* on concentration graph is sketch in Fig. 10. The more values of Nb increase, the more concentration graph increase, but the concentration boundary layer thickness decrease.

Table-4 shows the values of the skin-friction coefficient (*Cf*) for different values of Magnetic parameter (*M*), Porous medium parameter (*K*), Thermophoresis parameter (*Nt*), Brownian motion parameter (*Nb*), Lewis number (*Le*), Prandtl number (Pr) and Biot number (*Bi*). Increasing values of Magnetic parameter (*M*), Lewis number (*Le*) and Prandtl number decreases the skin-friction coefficient and the reverse effect is observed in case of increasing values of Porous medium parameter (*K*), Thermophoresis parameter (*Nt*), Brownian motion parameter (*Nb*) and Biot number (*Bi*).

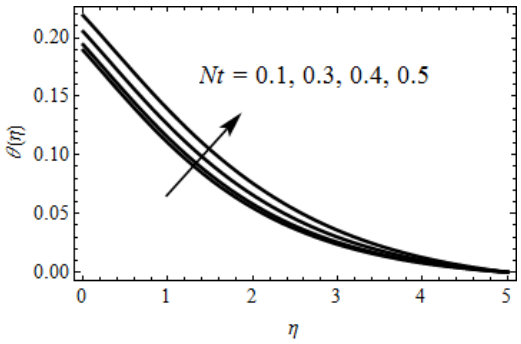

Fig. 5 *Nt* effect on Temperature profiles

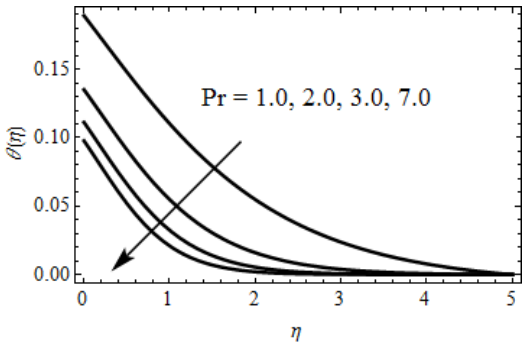

Fig. 6. Pr effect on Temperature profiles

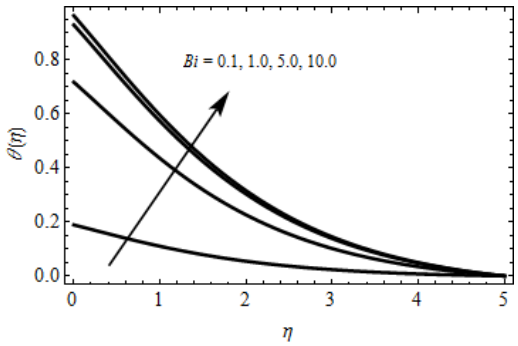

Fig.7 *Bi* effect on Temperature profiles

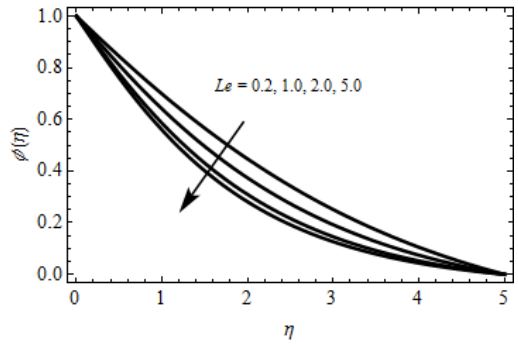

Fig. 8 *Le* effect on Concentration profiles

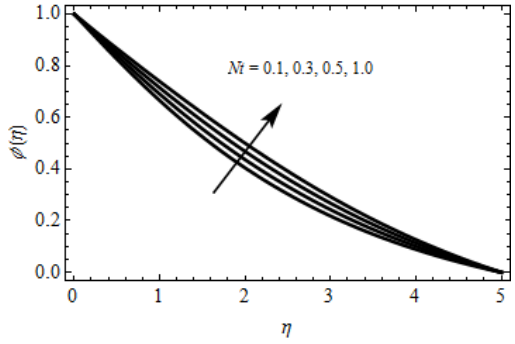

Fig.9 *Nt* effect on Concentration profiles

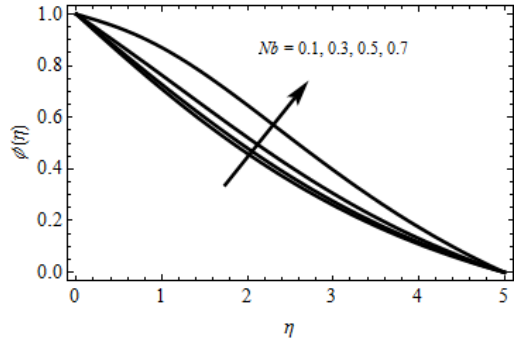

Fig.10 *Nb* effect on Concentration profiles

Table-5 presents the numerical values of Nusselt number or rate of heat transfer coefficient (Nu_x) for different values of Thermophoresis parameter (*Nt*), Brownian motion parameter (*Nb*), Prandtl number (Pr) and Biot number (*Bi*). Here, the Nusselt number increases for increasing values of Thermophoresis parameter (*Nt*), Brownian motion parameter (*Nb*), Biot number (*Bi*) whenthere is an increase in Prandtl number (Pr), it decreases.

Table-4.: Numerical values of the skin-friction coefficient (*Cf*) for variations of *M*, *K*, Pr, *Nb*, *Nt*, *Le* and *Bi*

M	*K*	Pr	*Nb*	*Nt*	*Le*	*Bi*	*Cf*
0.1	0.1	1.0	0.1	0.1	0.2	0.1	1.05223015426
0.4							0.95201325488
0.7							0.86231554655
0.1	**0.3**						1.11562884124
	0.5						1.15033247852
	0.1	**3.0**					0.92115483201
		5.0					0.82302665166
		0.1	**0.3**				1.09202155420
			0.5				1.12305660215
			0.1	**0.3**			1.08922315045
				0.5			1.11962331022
				0.1	**0.6**		0.96230014736
					0.8		0.89233215017
					0.2	**0.3**	1.10250015483
						0.5	1.15362265904

Table-5.: Numerical values of the Nusselt number (Nu_x) for variations of Pr, *Nb*, *Nt* and *Bi*

Pr	*Nb*	*Nt*	*Bi*	Nu_x
1.0	0.1	0.1	0.1	0.38550231547
3.0				0.32562201896
5.0				0.26302554778
1.0	**0.3**			0.43629551433
	0.5			0.46251148485
	0.1	**0.3**		0.42985012247
		0.5		0.46021588879
		0.1	**0.3**	0.45232658855
			0.5	0.48033261114

Table-6.: Numerical values of the Sherwood number (Sh_x) for variations of *Le*, *Nb* and *Nt*

Le	*Nb*	*Nt*	Sh_x
0.2	0.1	0.1	0.92132556548
0.6			0.86251147823
0.8			0.80621104578
0.2	**0.3**		0.98300215462
	0.5		1.05230015486
	0.1	**0.3**	0.97825510014
		0.5	1.04980225136

Table-6 presents the variation in Sherwood number or rate of mass transfer coefficient (Sh_x) due to the influence of Thermophoresis parameter (Nt), Brownian motion parameter (Nb) and Lewis number (Le). From this table, the Sherwood number is an increasing function of Thermophoresis parameter (Nt), Brownian motion parameter (Nb) when there is a decrease in the function of Lewis number (Le).

5. Conclusions

The boundary layer viscous flow and heat transfer of a non-newtoniannanofluid over a non-linearly stretching sheet in presence of variable viscosity and convective boundary condition effects is studied numerically. The influence of the governing parameters such as Magnetic parameter (M), Porous medium parameter (K), Thermophoresis parameter (Nt), Brownian motion parameter (Nb), Lewis number (Le), Prandtl number (Pr) and Biot number (Bi) on the velocity, temperature and nanoparticle concentration profiles are discussed graphically. The results are as follows:

1. When the magnetic parameter (M) raises, then it reduces the velocity profile due to the effect of Lorentz force.
2. By increasing the Brownian motion parameter (Nb), both the temperature and concentration profiles increase.
3. By increasing the values of the thermophoresis parameter (Nt), the temperature and concentration increase. As Le increases, the concentration decreases.
4. It is observed that the present results are equalized with the previous work done by Khan and Pop [7], Wang [16] and Gorla and Sidawi [3].

Acknowledgement: The authors are thankful to the Referee for valuable comments and suggestions.

References

[1] Aziz, A. (2009). A similarity solution for laminar thermal boundary layer over a flat plate with a convective surface boundary condition, *Commun. Nonlinear Sci. Numer. Simul.*, **14**, 1064-1068.

[2] Buongiorno, J. (2006). Convective transport in nanofluids, *J. Heat Transf.*, **128**, 240-250.

[3] Gorla, R. S. R. and Sidawi, I. (1994). Free convection on a vertical stretching surface with suction and blowing, *Appl. Sci. Res*. **52**, 247-257.

[4] Hayat, T., Aziz, A., Muhammad, T. and Ahmad, B. (2015). Influence of magnetic field in three-dimensional flow of couple stress nanofluid over a nonlinearly stretching surface with convective condition, *PLOS ONE*, **10**(12), p. e0145332.

[5] Ibanez, G. (2015). Entropy generation in MHD porous channel with hydrodynamic slip and convective boundary conditions, *Int. J. Heat Mass Transf.*, **80**, 274-280.

[6] Ishak, A. (2010). Similarity solutions for flow and heat transfer over a permeable surface with convective boundary condition, *Appl. Math. Comput.*, **217**, 837-842.

[7] Khan, W. A. and Pop, I. (2010). Boundary-layer flow of a nanofluid past a stretching sheet, *Int. J. Heat Mass Transf*., **53**, 2477-2483.

[8] López, A., Ibáñez, G., Pantoja, J., Moreira, J. and Lastres, O. (2017). Entropy generation analysis of MHD nanofluid flow in a porous vertical microchannel with nonlinear thermal radiation, slip flow and convective-radiative boundary conditions, *Int. J. Heat Mass Transf*., **107**, 982-994.

[9] Mahanthesha, B., Gireesha, B.J. and Gorla, R.S.R. (2016). Nonlinear radiative heat transfer in MHD three-dimensional flow of water based nanofluid over a non-linearly stretching sheet with convective boundary condition, *J. Niger. Math. Soc.*, **35**, 178-198.

[10] Mahanthesha, B., Gireesha, B.J. and Gorla, R.S.R. (2016). Nonlinear radiative heat transfer in MHD three-dimensional flow of water based nanofluid over a non-linearly stretching sheet with convective boundary condition, *J. Niger. Math. Soc.*, **35**, 178-198.

[11] Makinde, O. D. and Aziz, A. (2011). Boundary layer flow of a nanofluid past a stretching sheet with a convective boundary condition, *Int. J. Therm. Sci*., **50**, 1326-1332.

[12] Murali, E.M. Reddy and Narendra (2015). Heat and Mass Transfer with Free Convection MHD Flow past a Vertical porous Plate: Numerical study, *International Journal of Science and Engineering (IJSE)*, **8**, 95-103.

[13] Nadeem, S., Mehmood R. and Akbar, N. S. (2015). Partial slip effect on non-aligned stagnation point nanofluid over a stretching convective surface, *Chin. Phys. B*, **24** (1), 1-8.

[14] Paul, Ajit, Babu, NVN and Murali, Heat and mass transfer effects on an unsteady hydromagnetic free convective flow over an infinite vertical plate embedded in a porous medium with heat absorption, *Int. Journal of Open Problems in Computer Science and Mathematics*, **238**, 1-13.

[15] Reddy, Ch. Ram, Murthy, P. V. S. N., Chamkha, A. J. and Rashad, A. M. (2013). Soret effect on mixed convection flow in a nanofluid under convective boundary condition, *Int. J. Heat Mass Transf.*, **64**, 384-392.

[16] Wang, C.Y. (1989). Free convection on a vertical stretching surface, *J. Appl. Math. Mech*. (*ZAMM*) **69**, 418-420.